SNHG12 Regulated by KMT2B Participates in the Pathogenesis of Renal Cell Carcinoma via E2F1/CEP55

Jia-fu Feng (fengjiafu@uestc.edu.cn)
Department of Clinical Laboratory,Mianyang Central Hospital,School of Medicine,University of Electronic Science and Technology of China https://orcid.org/0000-0002-1714-4110

Jun Wang
Department of Medical Technology Institute,Chengdu University of Traditional Chinese Medicine

Gang Xie
Department of Pathology,Mianyang Central Hospital,School of Medicine,University of Electronic Science and Technology of China

Yao-dong Wang
Department of Urology Surgery,Mianyang Central Hospital,School of Medicine,University of Electronic Science and Technology of China

Xiao-han Li
Department of Medical Laboratory,Affiliated Hospital of Southwest Medical University

Wen-yu Yang
Department of Medical Technology Institute,Chengdu University of Traditional Chinese Medicine

Yu-wei Yang
Department of Clinical Labortory,Mianyang Central Hospital,School of Medicine,University of Electronic Science and Technology of China

Bin Zhang
Department of Clinical Laboratory,Mianyang Central Hospital,School of Medicine,University of Electronic Science and Technology of China

---

Research Article

Keywords: Renal cell carcinoma, long non-coding RNA, SNHG12, E2F1, CEP55

Posted Date: January 4th, 2022

DOI: https://doi.org/10.21203/rs.3.rs-1103258/v1

Abstract

Objective: This study is to investigate the regulation of long non-coding RNA (lncRNA) SNHG12 promoter methylation modification by KMT2B and the mechanism of SNHG12 in the development of renal cell carcinoma (RCC) involving E2F1/CEP55 axis.

Methods: TCGA and GEO databases were used to predict the involvement of SNHG12 in RCC. Knockdown of SNHG12/E2F1/CEP55 was performed. Next, SNHG12 expression and other mRNAs were analyzed by RT-qPCR. Subsequently, CCK-8 was used to detect cell proliferation. Wound healing test and Transwell assay was used to detect cell migration and invasion, respectively. The vascularization of HUVEC was explored by *in vitro* pseudotubule formation. CHIP was used to detect H3K4me3 in SNHG12 promoter region. The binding of E2F1 and CEP55 promoter region was analyzed with CHIP and dual luciferase reporter assay. RIP was used to detect the binding of SNHG12 and E2F1. Finally, the effect of SNHG12 on the tumor formation and angiogenesis of RCC was assessed in nude mouse xenograft model.

Results: Bioinformatics analysis showed that SNHG12 was highly expressed in RCC tissues and cells, and it was related to the poor prognosis of RCC patients. SNHG12 knockdown significantly inhibited RCC cell proliferation, migration, and invasion and HUVEC angiogenesis. KMT2B up-regulated SNHG12 through modifying H3K4me3 in its promoter region. In addition, SNHG12 promoted CEP55 expression by recruiting the transcription factor E2F1. Knockdown of SNHG12 blocked E2F1 recruitment, thereby down-regulating the expression of CEP55, and inhibited tumor formation and angiogenesis of RCC cells in nude mice.

Conclusion: KMT2B up-regulates SNHG12 via the modification of H3K4me3 in its promoter region. SNHG12 recruits E2F1 to promote the expression of CEP55, and ultimately promotes RCC cell proliferation, migration, and invasion and HUVEC angiogenesis.

Introduction

Renal cell carcinoma (RCC) is the main pathological type of kidney cancer, accounting for 70–90% [1]. Epidemiological survey shows that its morbidity and mortality have both been on the rise worldwide in recent years [2]. RCC is a highly concealed malignant tumor originating from the renal tubular epithelium. Only 10% of patients present with the “classic triad” (flank pain, gross hematuria, and a palpable renal mass) [3]. Due to the lack of biomarkers for early diagnosis and prognosis of RCC, most RCC patients are diagnosed at the middle and late stages, accompanied by local spread and distant metastasis [4]. The main treatment of RCC is radical or partial nephrectomy followed by chemotherapy and/or radiotherapy. In addition, 20% - 40% of patients have recurrence and/or distant metastasis after surgery. Although progresses have been made in the diagnosis and treatment of RCC in the past decades, RCC is still one of the most drug-resistant malignancies and a common cause of cancer-related deaths [5]. Therefore, it is urgent to explore the molecular mechanism of RCC occurrence and development, to identify new and reliable biomarkers of RCC and to develop new therapeutic targets for early diagnosis and treatment of RCC.

Long non-coding RNA (lncRNA) is a type of non-coding RNA with a length greater than 200 nucleotides. It is involved in the multi-level regulation of gene expression and its abnormal expression and mutation are

usually closely related to tumorigenesis and metastasis [6-8]. In addition, lncRNA can be specifically expressed in cancer and stably exist in body fluids [9-11], which can be used as a new type of cancer biomarkers and therapeutic targets. Some lncRNAs can encode small nucleolar RNA and are called small nucleolar RNA host genes (SNHGs). Of them, SNHG12 has been reported to be up-regulated in human endometrial cancer [12], bladder cancer [13], nasopharyngeal cancer [14], colorectal cancer [15], lung adenocarcinoma [16], breast cancer [17], liver cancer [18], and clear cell RCC [19], and plays an important role in proliferation and migration of cancer cells. The methylation of lncRNAs promoter can regulate expression of lncRNA, which is related to the occurrence of many diseases. For example, in clear cell RCC, the methylation status of two CpG sites is negatively correlated with the expression of SNHG3 and SNHG15, suggesting that DNA hypomethylation may play an important role in promoting the transcription of SNHG3 and SNHG15 [20]. SNHG11 binds to the HRE site in the gene promoter, and promotes gene transcription and tumor invasion and metastasis of colorectal cancer through the SNHG11/HIF-1α pathway [21]. CpG methylation in the promoter region of SNHG12 promotes the competitive binding of SNHG12 with miR-129-5p, regulates the MAPK/ERK pathway and G1/S cell cycle transition, thereby affecting the resistance of glioblastoma cells to temozolomide [22]. However, the role of SNHG12 regulated by DNA methylation in RCC is still unclear.

In this study, we explored the role of SNHG12 promoter methylation in RCC development through series loss- and gain-of-function experiments. Our findings may provide evidence for identifying new molecular targets for the diagnosis and treatment of RCC.

Materials And Methods

Bioinformatics analysis

The RNA sequencing data and corresponding clinical data of RCC tissue and normal tissue samples were downloaded from TCGA database through UCSC Xena (https://xena.ucsc.edu/). The GSE71963 dataset was obtained from GEO database (https://www.ncbi.nlm.nih.gov/gds). In total, we obtained 535 RCC tissue samples and 72 normal tissue samples from TCGA, as well as 32 RCC samples and 16 normal tissues samples from GSE71963 dataset. The R language “limma” package (http://www.bioconductor.org/packages/ release/bioc/html/limma.html) was used to screen differentially expressed lncRNAs, with |logFC|>1 and P <0.05. Kaplan-Meier survival analysis was performed using the R software “survival” package (http://bioconductor.org/packages/ survival/), with P<0.05. ENCORI database (http://starbase.sysu.edu.cn/index.php) was used for correlation analysis. LncMAP database (http://bio-bigdata.hrbmu.edu.cn/LncMAP/) was used to predict the transcription factors of SNHG12 regulating centrosome protein 55(CEP55) in RCC. The UCSC database (http://genome-asia.ucsc.edu/) was used to analyze the epigenetic modification of the SNHG12 promoter region.

Study cohort

RCC tissues and the corresponding precancerous tissue samples were collected from RCC patients (n=46) who were treated in Mianyang Central Hospital from January 2017 to January 2019. All patients were confirmed to have RCC by surgery and pathological analysis. The inclusion criteria: 1) Patients with

pathologically confirmed RCC cases; 2) Patient did not receive any chemotherapy, radiotherapy, or other antitumor treatment before operation; 3) Patients had complete clinical data. The exclusion criteria: 1) Patients without pathological confirmation; 2) Patients with recurrence and distant metastasis after treatment; 3) Patients with a history of mental illness; 4) Patients with dysfunction of the heart, liver, pancreas, and other important organs; 5) Patients with respiratory and circulatory diseases; 6) Patients with non RCC tumors. Prior written and informed consent were obtained from every patient and the study was approved by the Ethics Review Committee of Mianyang Central Hospital (P2020030).

Cell culture and transfection

HUVECs, purchased from Zhong Qiao Xin Zhou Biotechnology (DFSC-EC-01; Shanghai, China), were cultured at 37℃ with 5% CO_2 in endothelial cell basic medium containing fetal bovine serum (FBS) (Gibco, USA). RCC cell lines A498, 786-O, Caki-1, and 769-P, and human normal kidney cell line HK-2 purchased from ATCC (MA, USA) were cultured in modified Eagle medium (Gibco) containing 10.0% FBS (Gibco) and 1.0% antibiotics (100U/mL penicillin and 100 mg/mL streptomycin).

Cells were transfected with plasmids of sh-SNHG12 (short hairpin RNA-SNHG12), oe-SNHG12 (SNHG12 overexpression), sh-KMT2B, oe-E2F1, oe-SNHG12 + sh-E2F1, sh-E2F1 + oe-CEP55, using Lipofectamine 2000 (Invitrogen, Carlsbad, CA, USA). Corresponding negative control (NC) groups were set up. The plasmids were all constructed by GenePharma Co., Ltd. (Shanghai, China), and the plasmid concentration was 50 ng/ml. The shRNA sequences are listed as follows: sh-SNHG12 (1: TGATCCTGAGGAGGTGAGCTTGTTT; 2: GAGCTGTGCTTTAAGATTCATGTTA; 3: GCTGTGCTTTAAGATTCATGTTACA) ; sh-KMT2B (1: AGTCTCAGTATCTCACTCCTA; 2: GCCTTCAGAAATTGTGGATTT; 3: CGGTGCCGAATTCTAGAGTAT); sh-E2F1 (1: TAACTGCACTTTCGGCCCTTT; 2: CATCCAGCTCATTGCCAAGAA; 3: TAAGAGCAAACAAGGCCCGAT) .

CCK-8

After 48 h of transfection, cells were seeded into 96-well plates at 1.0×10^5 cells/ml (100 μL/well). After routine culture overnight, the cells were treated according to CCK-8 kit (Beyotime, Shanghai, China), and the cell viability was detected at 24 h, 48 h, and 72 h. The OD490 was detected with a microplate reader.

Wound healing test

The cells were seeded in a 6-well plate at 2.5×10^4 cells/ml and cultured for 24 h. Next, a 10 μL sterile disposable pipette was used to make a scratch on the cells. The cell images at 0 h and 48 h after the scratch were taken under an inverted microscope. The relative distance of cell migration to scratch area was measured, and the actual migration distance was calculated according to the scratch area distance of cells.

Transwell assay

The Transwell upper chamber (Yanhui Biotechnology, Shanghai, China) was pre-coated with ECM gel (Sigma-Aldrich, USA). After starving culture for 24 h, the cells were added to the upper chamber at 2.5×10^5 cells/ml (0.2 ml in total). In the lower chamber, 700 μL of pre-cooled DMEM medium containing 10% FBS was added. The chamber was then incubated in a 37°C, 5% CO_2 saturated humidity incubator. After 24 h, the cells in the lower chamber were fixed with methanol, stained with 0.1% crystal violet. Invaded cells were photographed

and counted using randomly selected 5 visual fields in each chamber under an inverted microscope with a magnification of 200 ×. The experiment was repeated three times independently.

Matrigel-based capillary-like tube formation in vitro

RCC cells were transfected as above described. After 48 h, the cell supernatant was collected. The tumor-conditioned medium was prepared according to the ratio of 4:5:1 (tumor supernatant: DMEM medium: FBS). HUVECs were seeded into a 96-well plate pre-coated with Matrigel and incubated with tumor-conditioned medium for 8 h. Finally, 4 fields of view were randomly selected from each well and the tube length was quantified under the phase-contrast microscope.

Chromatin immunoprecipitation (ChIP)

786-O cells transfected with sh-NC or sh-KMT2B were fixed with 1.0% formaldehyde and subjected to ultrasonic treatment to obtain the DNA fragments. For ChIP, the supernatant was incubated with the negative control antibody rabbit anti-IgG (ab109489, 1:100), H3K4me3 antibody (1: 1000, ab8580), and E2F1 antibody (1: 500, ab179445) (Abcam, Cambridge, UK) at 4°C overnight. The endogenous DNA-protein complexes were precipitated with Protein Agarose/Sepharose (Sangon biotech, Shanghai, China). The DNA fragments were extracted with phenol/chloroform. RT-qPCR was used to detect the enrichment of H3K4me3 in the SNHG12 promoter and E2F1 in the CEP55 promoter.

RNA immunoprecipitation (RIP)

RIP kit (Millipore, USA) was used to detect the binding of SNHG12 and E2F1 protein. The 786-O cells were subjected to lysis with RIPA (P0013B, Beyotime) for 5 min. The antibody-bound magnetic beads, which were prepared by incubating magnetic beads with anti-E2F1 (1:50, ab179445, Abcam) and IgG (ab172730, 1:100, Abcam) for 30 min, were incubated with the supernatant at 4°C overnight. After that, the samples were digested with proteinase K and RNA was extracted for subsequent RT-qPCR detection.

Dual luciferase reporter assay

The potential binding site of E2F1 in the promoter region of CEP55 was analyzed through the bioinformatics website (http://jaspar.genereg.net). After that, the pGL3- CEP55-WT and pGL3-CEP55-MUT plasmids were constructed with wild type (WT) and mutant type (MUT) binding sequences of E2F1, respectively. Then, these plasmids were co-transfected with oe-NC and oe-E2F1 into the HEK-293T cells (ATCC). After 48 h, the Dual-Luciferase Reporter Assay System kit (Promega, USA) and the TD-20/20 Luminometer was used to detect the luciferase activity.

RT-qPCR

The nucleus and cytoplasm of RCC cells were separated using PARIS kit (Life Technologies, Carlsbad, CA, USA). The total RNA of cells and tissues as well as nucleus and cytoplasm of RCC cells was extracted by Trizol (Invitrogen). RT-qPCR was conducted as reported previously [24]. The primers are shown in Table 1.

Table 1
RT-qPCR primers.

Targets	Primer sequences
KMT2B (human)	F: 5'-TGACAAGTGTGAATCCCGTGAAG-3'
	R: 5'-AACCATTTCATCCGTTGTTACGAAG-3'
SNHG12 (human)	F: 5'-TCTGGTGATCGAGGACTTCC-3'
	R: 5'-ACCTCCTCAGTATCACACACT-3'
E2F1 (human)	F: 5'-ATGTTTTCCTGTGCCCTGAG-3'
	R: 5'-ATCTGTGGTGAGGGATGAGG-3'
CEP55 (human)	F: 5'-AGTAAGTGGGGATCGAAGCCT-3'
	R: 5'-CTCAAGGACTCGAATTTTCTCCA-3'
GAPDH (human)	F: 5'-GGAGCGAGATCCCTCCAAAAT-3'
	R: 5'-GGCTGTTGTCATACTTCTCATGG-3'
Note: F, forward; R, reverse.	

Western Blot

The total protein of tissues or cells was extracted with RIPA (P0013B, Beyotime). Protein concentration was determined using BCA kit (ThermoFisher Scientific, USA). After separation by polyacrylamide gel electrophoresis, the proteins were transferred to PVDF membrane and blocked with 5% BSA for 1 h. The detailed experimental method was similar to previous reports [24].

Nude Mouse Xenograft Model

BALB/c female nude mice (n=30; 3-4 weeks old; J004, Nanjing Junke Bioengineering Co., Ltd., Jiangsu, China) were randomly grouped and inoculated with 786-O cells (0.1 ml; 2×10^7 cells/ml) stably transfected with different plasmids, including sh-SNHG12 + oe-E2F1, sh-E2F1 + oe-CEP55, and corresponding NC plasmids. The tumor volume was measured weekly. The tumor volume was calculated by length×width^2×0.5. Five weeks after inoculation, mice were euthanized by intraperitoneal injection of overdose pentobarbital sodium (100mg/kg). The tumors were dissected, the tumor volume was observed, and the tumor weight was measured. All animal experiments were conducted according to the ethical guidelines of Ethics Review Committee of Mianyang Central Hospital (P2020030). All efforts were made to minimize animal suffering.

Immunohistochemistry

Paraffin sections of tumor tissues were dewaxed, alcohol gradient dehydrated, and rehydrated. The sections were incubated with VEGF antibody (ab72807, 1:50) at 4°C overnight. After that, sections were incubated with goat anti-rabbit IgG secondary antibody (ab150077, 1:100), developed with DAB, and counterstained with hematoxylin. The results were evaluated by two experienced pathologists in a blinded manner. The

positive rate of VEGF was calculated as the ratio of positive cells to total number of cells. Specific experiment was similar to previous reports [24, 25].

Statistical analysis

All data were analyzed using SPSS21.0, and expressed as Mean ± SD. The paired two groups were compared by paired t test. One-way ANOVA was used for data comparison among multiple groups. Tukey's test was used for post-hoc test. The OD value at different time points was compared using two-way ANOVA. Tumor sizes at different time points were analyzed by repeated measures ANOVA, and Bonferroni was used for post-hoc test. The count data was compared with fourfold table Chi-square test. $P < 0.05$ indicated that the difference was statistically significant.

Results

SNHG12 is up-regulated in RCC

Through bioinformatics analysis, 170 differentially expressed lncRNAs were detected in TCGA database (105 highly expressed and 65 poorly expressed) (Figure 1A), and 24 differentially expressed lncRNAs were obtained in GSE71963 datasets (11 highly expressed and 13 poorly expressed) (Figure 1B). Then, we overlapped the highly expressed lncRNAs in TCGA database and GSE71963 datasets and screened out 5 lncRNAs that were highly expressed in RCC (Figure 1C). However, further survival analysis showed that only SNHG12 was associated with poor prognosis of RCC (Figure 1D). Next, compared with paracancerous tissues (0.998 ± 0.163), SNHG12 was upregulated ($t=34.837$, $p<0.001$) in RCC tissues (4.066 ± 0.628) (Figure 1E). In addition, SNHG12 had no significant relation with patient sex ($\chi^2 = 0.383$, $p=0.536$) and age ($\chi^2 = 0.090$, $p=0.765$), but had significant association with tumor grade ($\chi^2 = 9.217$, p□0.006), TNM stage ($\chi^2 = 5.254$, $p=0.047$), and lymph node metastasis ($\chi^2 = 5.855$, $p=0.035$) (Table 2). Compared with HK-2 cells, RCC cell lines (A498, 786-O, Caki-1, and 769-P) had up-regulated SNHG12 (Figure 1F). Of note, SNHG12 level was highest in 786-O cells ($q=18.530$, $p<0.001$).

Table 2
Relationship between SNHG12 level and clinicopathological characteristics of RCC patients.

Items	N	SNHG12 level		*P* value
		High	Low	
Age				0.765
<60	27	14	13	
≥60	19	9	10	
Gender				0.536
Male	30	16	14	
Female	16	7	9	
TNM stage				0.047
I-II	33	13	20	
III-IV	13	10	3	
Fuhrman grade				0.006
G1-2	28	9	19	
G3	18	14	4	
Lymph node metastasis				0.035
Yes	11	9	2	
No	35	14	21	

Note: The data was analyzed by Chi-square test. However, if T<5, the data was further analyzed by Fisher's method.

SNHG12 knockdown inhibits proliferation, migration, and invasion of RCC cells and HUVEC angiogenesis

SNHG12 WAS knocked down by shRNA in RCC cell line 786-O, RT-qPCR showed that sh-SNHG12-1 had the highest knockdown efficiency (Figure 2A) and was thus used for subsequent experiments.

Next, CCK-8 showed that compared with the control, SNHG12 knockdown inhibited cell proliferation after incubation for 48h (t=5.850, p=0.002) and 72h (t=11.128, p<0.001), as revealed by decreased OD490 value (Figure 2B). In addition, wound healing test showed that knockdown of SNHG12 decreased migration distance (t=6.625, p=0.003), indicating inhibited migration ability (Figure 2C). Transwell assay showed that knockdown of SNHG12 inhibited invasion of RCC cells (t=6.636, p=0.003) (Figure 2D). In addition, *in vitro* capillary-like tube formation experiments showed that knocking down SNHG12 inhibited capillary-like tube formation, thus suppressing HUVEC angiogenesis (t=8.476, p=0.001) (Figure 2E). Western Blot showed that

knocking down SNHG12 inhibited protein levels of MMP-2 (t=7.551, p=0.002), MMP-9 (t=6.674, p=0.003), and VEGF (t=6.864, p=0.002) (Figure 2F).

KMT2B up-regulates SNHG12 by regulating the H3K4me3 modification of the SNHG12 promoter

As shown in Figure 3A, there was a large amount of H3K4me3 enrichment in the SNHG12 promoter. It is reported that KMT2B mediates the transcriptional activation of H3K4me3 modification [26]. Moreover, through ENCORI database analysis, KMT2B was highly expressed in RCC (Figure 3B) and positively correlated with SNHG12 expression (Figure 3C). Therefore, KMT2B may regulate SNHG12 by mediating the H3K4me3 modification of its promoter region.

KMT2B mRNA (t = 32.217, P < 0.001) and protein expression (t = 26.836, p<0.001) increased in RCC tissues compared with adjacent tissues (Figure 3D). Compared with human normal kidney cell line HK-2, KMT2B (A498: q=8.968, p<0.001; 786-O: q=18.341, p<0.001; Caki-1: q=9.740, p<0.001; 769-P: q=4.657, p=0.049) and protein expression (A498: q=11.443, p<0.001; 786-O: q=17.322, p<0.001; Caki-1: q=8.446, p<0.001; 769-P: q=5.656, p=0.017) in RCC cells was increased (Figure 3E). Next, we knocked down KMT2B in 786-O cells and found reduced SNHG12 expression (t=11.509, p<0.001) (Figure 3F). ChIP showed that knocking down KMT2B reduced modification of SNHG12 promoter H3K4me3 (t=11.413, p<0.001) (Figure 3G).

SNHG12 recruits E2F1 to promote CEP55 expression

In RCC, SNHG12 was positively correlated with CEP55 expression (r=0.234, p<0.001) (Figure 4A), which is highly expressed in RCC and can promote cancer cell proliferation, invasion, and migration [24]. Analysis with LncMAP database showed that E2F1 was one of the transcription factors involved in regulation of SNHG12 on CEP55 in RCC (Table 3). Additionally, ENCORI database analysis showed that E2F1 was highly expressed in RCC (Figure 4B) and positively correlated with CEP55 (r=0.542, p<0.001) (Figure 4C). Therefore, SNHG12 may regulate CEP55 through E2F1.

Table 3
The transcription factors of SNHG12 regulating CEP55 in RCC predicted by LncMAP.

LncRNA Symbol	TF Symbol	Gene Symbol
SNHG12	E2F1	CEP55
SNHG12	PBX3	CEP55

To further verify this hypothesis, we showed that SNHG12 was mainly located in the nucleus (Figure 4D). RIP results showed enriched SNHG12 when using anti-E2F1 antibody (t=11.889, p<0.001) (Figure 4E). Meanwhile, CEP55 promoter region was bound by anti-E2F1 antibody (t=9.566, p<0.001) (Figure 4F). Furthermore, overexpression of SNHG12 promoted binding of E2F1 with CEP55 promoter region, whereas SNHG12 inhibited this binding (oe-NC *vs.* oe-SNHG12: q=8.724, p=0.001; sh-NC *vs.* sh-SNHG12: q=11.861, p<0.001) (Figure 4G). Then, we predicted the binding site between E2F1 and CEP55 promoter region through Jaspar (Table 4). Dual luciferase reporter assay showed that the truncation or mutation of site 1 did not

affect the luciferase activity of the oe-E2F1 group, while sites 2 and 3 were mutated, the luciferase activity increased (Figure 4H and 4I). The above results revealed that site 1 was the main site for E2F1 to act on the CEP55 promoter region.

Table 4
JASPAR analysis of the binding site of the E2F1 in the promoter region of CEP55.

Matrix ID	Name	Score	Relative score	Sequence ID	Start	End	Strand	Predicted sequence
MA0024.1	E2F1	7.17655	0.813289007993	CEP55	292	299	+	tttgcccc
MA0024.1	E2F1	7.17655	0.813289007993	CEP55	1091	1098	-	ttagccgc
MA0024.1	E2F1	6.81352	0.800797328565	CEP55	836	843	-	tttcccga

Finally, in the 786-O cells, CEP55 expression was increased by SNHG12 overexpressing (q=20.319, p<0.001), but reduced by further silencing E2F1 (q=6.508, p=0.008). When overexpressing SNHG12 and silencing E2F1 at the same time, CEP55 expression was reduced (q=19.571, p<0.001) (Figure 4J).

SNHG12 recruits E2F1 to promote RCC cell proliferation, migration, and invasion and HUVEC angiogenesis

Compared with oe-SNHG12 + sh-NC, E2F1 (q=11.902, p<0.001) and CEP55 (q=9.059, p<0.001) expression were decreased by oe-SNHG12 + sh-E2F1. Compared with sh-E2F1 + oe-NC, E2F1 expression remained not changed by sh-E2F1 + oe-CEP55 treatment (q=0.592, p=0.974), but CEP55 expression was elevated (q=7.761, p=0.003) (Figure 5A).

In addition, compared with the oe-SNHG12 + sh-NC group, cell proliferation ability (24h: q=0.904, p=0.918; 48h: q=9.545, p<0.001; 72h: q=18.003, p<0.001), cell migration and invasion ability (q=11.362, p<0.001; q=9.652, p<0.001), and capillary-like tube formation ability (q=8.552, p<0.001) of the oe-SNHG12 + sh-E2F1 group were decreased, while compared with the sh-E2F1 + oe-NC group, cell proliferation ability (24h: q=1.193, p=0.833; 48h: q=6.435, p=0.001; 72h: q=9.255, p<0.001), cell migration and invasion ability (q=5.429, p=0.021; q=7.011, p=0.005), and capillary-like tube formation ability (q=7.126, p=0.003) of the sh-E2F1 + oe-CEP55 group were increased (Figure 5B-E). The protein expression of MMP-2 (q=11.187, p<0.001), MMP-9 (q=11.251, p<0.001), and VEGF (q=15.538, p<0.001) in the oe-SNHG12 + sh-E2F1 group decreased compared with the oe-SNHG12 + sh-NC group, while the trend was opposite in the sh-E2F1 + oe-CEP55 group compared with the sh-E2F1 + oe-NC group (MMP-2: q=6.789, p=0.006; MMP-9: q=8.884, p=0.001; VEGF: q=8.970, p=0.001) (Figure 5F).

Knockdown of SNHG12 inhibits RCC growth and angiogenesis in vivo

As shown in Figure 6A-6C, compared with the NC, SNHG12 silencing slowed down tumor growth (3w: q=13.128, 4w: q=22.341, 5w: q=31.637, all p<0.001) and reduced tumor weight (q=16.945, p<0.001), while further E2F1 overexpression boosted tumor growth (3w: q=19.778, 4w: q=28.276, 5w: q=38.723, all p<0.001) and increased tumor weight (q=15.807, p<0.001). Compared with silencing E2F1 alone, simultaneous silencing E2F1 and overexpressing CEP55 enhanced tumor growth (3w: q=19.956, 4w: q=24.591, 5w: q=38.692, all p<0.001) and weight (q=20.071, p<0.001) .

Compared with NC, silencing SNHG12 reduced E2F1 (q=29.522, p<0.001) and *CEP55* (q=19.445, p<0.001) expression, while further E2F1 overexpression reversed this trend (E2F1: q=26.221, p<0.001; CEP55: q=20.545, p<0.001). Compared with silencing E2F1 alone, simultaneous silencing E2F1 and overexpressing CEP55 up-regulated *CEP55* (q=27.005, p<0.001) (Figure 6D).

Immunohistochemical detection showed that compared with NC, silencing SNHG12 decreased VEGF protein expression (q=15.484, p<0.001), which was reversed by further E2F1 overexpression (q=17.701, p<0.001). Compared with silencing E2F1 alone, simultaneous silencing E2F1 and overexpressing CEP55 increased VEGF expression (q=22.056, p<0.001) (Figure 6E). Meanwhile, compared with NC, silencing SNHG12 reduced MMP-2 (q=24.073, p<0.001), MMP-9 (q=23.464, p<0.001), VEGF (q=22.801, p<0.001) protein expression, which was neutralized by further E2F1 up-regulation(MMP-2: q=13.062, p<0.001; MMP-9: q=14.071, p<0.001; VEGF: q=15.967, p<0.001). Compared with silencing E2F1 alone, their expression was promoted after simultaneous silencing E2F1 and overexpressing CEP55 (MMP-2: q=15.733, p<0.001; MMP-9: q=16.792, p<0.001; VEGF: q=14.292, p<0.001) (Figure 6F).

Discussion

RCC is a heterogeneous tumor that originates from the renal parenchyma and is one of the deadliest malignant tumors in the urinary system [27]. So far, the mechanism underlying the occurrence and development of RCC is still not fully understood. RCC-related biomarkers are less studied, and RCC early diagnosis is difficult. In addition, RCC responds poorly to conventional chemotherapy and radiotherapy, and there is a lack of targeted therapy drugs for RCC, resulting in a poor prognosis and a low 5-year survival rate for RCC patients with advanced stage IV and later [28]. However, if diagnosed early, patients with local RCC can be treated by nephrectomy (partial or total nephrectomy). The treatment effect of TI and T2 stage surgery is better, which can not only improve the quality of life, but also the 5- to 10-year survival rate of RCC patients [29]. Therefore, further understanding of the pathogenesis of RCC may help the diagnosis and treatment of RCC patients. Here, in this study, we explored the regulation of SNHG12 by KMT2B and the downstream factors of SNHG12 (including E2F1 and CEP55) involved in its effect on RCC.

SNHG12 exerts a carcinogenic effect in a variety of cancers [12-20, 30-32]. In clear cell RCC, SNHG12, as a competitive endogenous RNA, competes with miR-30a-5p to bind downstream oncogenes RUNX2, IGF-1R and WNT2 to promote tumor cell invasiveness [33]. SNHG12, as a sponge of miR-129-5p, regulates the expression of MDM4 (a regulatory factor in p53 pathway) and p53 pathway during the development of clear cell RCC [34]. In addition, SNHG12 up-regulates CDCA3 by stabilizing the transcription factor SP1, thereby regulating the SNHG12/SP1/CDCA3 pathway to promote the proliferation, migration, invasion, and drug resistance of RCC [35]. SNHG12 also regulates HIF1α by competing with miR-199a-5p, thereby promoting its carcinogenic potential. However, SNHG12 deletion inhibits cell viability, anchorage-independent growth and induces apoptosis. Silencing SNHG12 can inhibit RCC cell migration and invasion *in vitro*, and inhibit growth of xenograft tumors *in vivo* [36]. In addition, SNHG12 can up-regulate its target gene COL11A1 (collagen type XI α1 chain) through microRNA-200c-5p, indicating that the SNHG12/miR-200c-5p/COL11A1 axis is crucial to the progress of RCC [37].

Here, in this study, the biological function and mechanism of SNHG12 in the occurrence and development of RCC were investigated. We first found that SNHG12 was highly expressed in RCC tissues and cells. In addition, the high expression of SNHG12 was related to tumor grade and poor prognosis of patients, and the expression of SNHG12 in the tissues of informed RCC patients was related to tumor grade, TNM staging, and lymph node metastasis. To further explore the effect of SNHG12 on the biological functions of RCC cells, we knocked down SNHG12 in 786-O and found that SNHG12 knockdown inhibited cell proliferation, migration, and invasion of RCC and HUVEC angiogenesis. A meta-analysis showed that high SNHG12 expression in a variety of tumors reduced the overall survival rate and recurrence-free survival rate of tumor patients and that the high expression of SNHG12 suggested unfavorable clinicopathological results, including larger tumors, lymph node metastasis, distant metastasis, and later clinical staging [38]. To further reveal the mechanism of high expression of SNHG12 in RCC, we searched the UCSC database and found that the promoter region of SNHG12 was enriched in H3K4me3. Next, we tested the enrichment of H3K4me3 in the promoter region of SNHG12 through ChIP and found that KMT2B up-regulated the expression of SNHG12 by mediating the modification of H3K4me3 in the promoter region of SNHG12. In addition, we predicted the possible binding sites of E2F1 and CEP55 promoter regions, and knocked down E2FF1 to explore the downstream factors of SNHG12 in RCC. We found that in RCC cells, SNHG12 overexpression promoted CEP55 expression by recruiting E2F1. Finally, we constructed a nude mouse xenograft tumor model. It was found that SNHG12 knockdown blocked the recruitment of E2F1 by SNHG12, and then down-regulated CEP55, leading to the inhibition of RCC growth and angiogenesis. Our results confirmed that the SNHG12/E2F1/CEP55 axis affected RCC growth and angiogenesis.

Conclusion

In summary, KMT2B up-regulates SNHG12 through the modification of H3K4me3 in the SNHG12 promoter region, which in turn recruits the transcription factor E2F1, and ultimately promotes expression of CEP55, and the proliferation, migration, and invasion of RCC cells, as well as the angiogenesis ability of HUVECs (Figure 7). These all ultimately promote RCC growth and angiogenesis.

Abbreviations

renal cell carcinoma (RCC), long non-coding RNA (lncRNA), small nucleolar RNA host gene 12 (SNHG12), E2F transcription factor 1 (E2F1), cell counting kit-8 (CCK-8), centrosome protein 55 (CEP55), chromatin immunoprecipitation (ChIP), RNA immunoprecipitation (RIP), real time quantitative PCR (RT-qPCR), sh-(short hairpin RNA-), oe-(overexpression-), negative control (NC), KMT2B (lysine methyltransferase 2B), vascular endothelial growth factor(VEGF), Analysis of Variance (ANOVA), human umbilical vein endothelial cells (HUVEC), matrix metalloproteinase (MMP)

Declarations

Acknowledgements

We would like to give our sincere appreciation to the reviewers for their helpful comments on this .

Funding

This work was supported by the Science and Technology Department of Sichuan Province (2015SZ0117, 2019YJ0701, and 2021YJ0239).

Authors' contributions

Conception and design of research: JFF, JW; Collected and assembled data: GX, YDW, YWY; Bioinformatics analysis: JW, XHL, YWY; Analyzed and interpreted data: XHL, WYY, JFF, BZ; Prepared figures: JW, YWY; Drafted manuscript: JFF, JW, YWY; Approved final version of manuscript: JFF, JW, GX, YDW, XHL, WYY, YWY, BZ.

Ethics approval and consent to participate

All research procedures were conducted with approval of the Ethics Committee of Mianyang Central Hospital and in line with the Declaration of Helsinki. All patients and/or legal guardians signed the informed consent documentation prior to experiments. Additionally, all animal experiments were approved by the Animal Ethics Committee of Mianyang Central Hospital. Great efforts were made to minimize the number of animals used in the experiments and their suffering.

Consent for publication

Not applicable.

Competing interests

All authors declare no financial competing interests.

All authors declare no non-financial competing interests.

Data availabilty statement

The datasets used and/or analysed during the current study are available from the corresponding author on reasonable request.

References

1. Siegel RL, Miller KD, Fuchs HE, Jemal A. Cancer Statistics 2021. CA Cancer J Clin. 2021; 71:7-33.
2. Liu X, Yu Y, Wang M, et al. Age-period-cohort analysis of kidney cancer deaths attributable to high body-mass index in China and U.S. adults. BMC Public Health. 2020; 20:882.
3. Moch H, Humphrey PA, Ulbright TM, Reuter VE. WHO Classification of Tumours of the Urinary System and Male Genital Organs. 4th ed. Lyon, France: IARC Press; 2016.

4. Capitanio U, Bensalah K, Bex A, et al. Epidemiology of Renal Cell Carcinoma. Eur Urol. 2019; 75:74-84.
5. Chen S, Ye H, Gong F, et al. Ginsenoside compound K exerts antitumour effects in renal cell carcinoma via regulation of ROS and lncRNA THOR. Oncol Rep. 2021; 45:38.
6. Statello L, Guo CJ, Chen LL, Huarte M. Gene regulation by long non-coding RNAs and its biological functions. Nat Rev Mol Cell Biol. 2021; 22:96-118.
7. Liang Y, Song X, Li Y, et al. LncRNA BCRT1 promotes breast cancer progression by targeting miR-1303/PTBP3 axis. Mol Cancer. 2020; 19:85.
8. Xing C, Sun SG, Yue ZQ, Bai F. Role of lncRNA LUCAT1 in cancer. Biomed Pharmacother. 2021; 134:111158.
9. Wang Y, Zhang D, Zhang C, Sun Y. The Diagnostic and Prognostic Value of Serum lncRNA NEAT1 in Colorectal Cancer. Cancer Manag Res. 2020; 12:10985-10992.
10. Tao Y, Tang Y, Yang Z, et al. Exploration of Serum Exosomal LncRNA TBILA and AGAP2-AS1 as Promising Biomarkers for Diagnosis of Non-Small Cell Lung Cancer. Int J Biol Sci. 2020; 16:471-482.
11. Xu W, Zhou G, Wang H, et al. Circulating lncRNA SNHG11 as a novel biomarker for early diagnosis and prognosis of colorectal cancer. Int J Cancer. 2020; 146:2901-2912.
12. Cai P, Wu M, Zhang B, et al. Long non coding RNA SNHG12 regulates cell proliferation, invasion and migration in endometrial cancer by targeting miR 4429. Mol Med Rep. 2020; 22:2842-2850.
13. Qing L, Gu P, Liu M, et al. Extracellular Matrix-Related Six-lncRNA Signature as a Novel Prognostic Biomarker for Bladder Cancer. Onco Targets Ther. 2020; 13:12521-12538.
14. Liu ZB, Tang C, Jin X, et al. Increased expression of lncRNA SNHG12 predicts a poor prognosis of nasopharyngeal carcinoma and regulates cell proliferation and metastasis by modulating Notch signal pathway. Cancer Biomark. 2018; 23:603-613.
15. Liao Q, Chen L, Zhang N, et al. Network analysis of KLF5 targets showing the potential oncogenic role of SNHG12 in colorectal cancer. Cancer Cell Int. 2020; 20:439.
16. Zhang H, Wang Y, Lu J. Identification of lung-adenocarcinoma-related long non-coding RNAs by random walking on a competing endogenous RNA network. Ann Transl Med. 2019; 7:339.
17. Zhang S, Ma F, Xie X, Shen Y. Prognostic value of long non-coding RNAs in triple negative breast cancer: A PRISMA-compliant meta-analysis. Medicine (Baltimore). 2020; 99:e21861.
18. Chen PP, Zhang ZS, Wu JC, et al. LncRNA SNHG12 promotes proliferation and epithelial mesenchymal transition in hepatocellular carcinoma through targeting HEG1 via miR-516a-5p. Cell Signal. 2021; 84:109992.
19. Yu H, Liu J, Zhang Z, et al. SNHG12 promotes carcinogenesis of human renal cell cancer via functioning as a competing endogenous RNA and sponging miR-30a-3p. J Cell Mol Med. 2021; 25:4696-4708.
20. Yang W, Zhang K, Li L, et al. Discovery and validation of the prognostic value of the lncRNAs encoding snoRNAs in patients with clear cell renal cell carcinoma. Aging (Albany NY). 2020; 12:4424-4444.
21. Xu L, Huan L, Guo T, et al. LncRNA SNHG11 facilitates tumor metastasis by interacting with and stabilizing HIF-1α. Oncogene. 2020; 39:7005-7018.

22. Lu C, Wei Y, Wang X, et al. DNA-methylation-mediated activating of lncRNA SNHG12 promotes temozolomide resistance in glioblastoma. Mol Cancer. 2020; 19:28.
23. Mummler C, Burgy O, Hermann S, et al. Cell-specific expression of runt-related transcription factor 2 contributes to pulmonary fibrosis. FASEB J. 2018; 32:703-716.
24. Feng J, Guo Y, Li Y, et al. Tumor promoting effects of circRNA_001287 on renal cell carcinoma through miR-144-targeted CEP55. J Exp Clin Cancer Res. 2020; 39:269.
25. Cheng R, Chen Y, Zhou H, et al. B7-H3 expression and its correlation with clinicopathologic features, angiogenesis, and prognosis in intrahepatic cholangiocarcinoma. APMIS. 2018; 126:396-402.
26. Hanna CW, Taudt A, Huang J, et al. MLL2 conveys transcription-independent H3K4 trimethylation in oocytes. Nat Struct Mol Biol. 2018; 25:73-82.
27. Bai X, Yi M, Dong B, et al. The global, regional, and national burden of kidney cancer and attributable risk factor analysis from 1990 to 2017. Exp Hematol Oncol. 2020; 9:27.
28. Padala SA, Barsouk A, Thandra KC, et al. Epidemiology of Renal Cell Carcinoma. World J Oncol. 2020; 11:79-87.
29. Zhang Y, Long G, Shang H, et al. Comparison of the oncological, perioperative and functional outcomes of partial nephrectomy versus radical nephrectomy for clinical T1b renal cell carcinoma: A systematic review and meta-analysis of retrospective studies. Asian J Urol. 2021; 8:117-125.
30. Wang C, Shao S, Deng L, et al. LncRNA SNHG12 regulates the radiosensitivity of cervical cancer through the miR-148a/CDK1 pathway. Cancer Cell Int. 2020; 20:554.
31. Cao W, Zhou G. LncRNA SNHG12 contributes proliferation, invasion and epithelial-mesenchymal transition of pancreatic cancer cells by absorbing miRNA-320b. Biosci Rep. 2020; 40:BSR20200805.
32. Qian M, Ling W, Ruan Z. Long non-coding RNA SNHG12 promotes immune escape of ovarian cancer cells through their crosstalk with M2 macrophages. Aging (Albany NY). 2020; 12:17122-17136.
33. Yu H, Liu J, Zhang Z, et al. SNHG12 promotes carcinogenesis of human renal cell cancer via functioning as a competing endogenous RNA and sponging miR-30a-3p. J Cell Mol Med. 2021; 25:4696-4708.
34. Wu Z, Chen D, Wang K, et al. Long Non-coding RNA SNHG12 Functions as a Competing Endogenous RNA to Regulate MDM4 Expression by Sponging miR-129-5p in Clear Cell Renal Cell Carcinoma. Front Oncol. 2019; 9:1260.
35. Liu Y, Cheng G, Huang Z, et al. Long noncoding RNA SNHG12 promotes tumour progression and sunitinib resistance by upregulating CDCA3 in renal cell carcinoma. Cell Death Dis. 2020; 11:515.
36. Chen Q, Zhou W, Du SQ, et al. Overexpression of SNHG12 regulates the viability and invasion of renal cell carcinoma cells through modulation of HIF1alpha. Cancer Cell Int. 2019; 19:128.
37. Xu C, Liang H, Zhou J, et al. lncRNA small nucleolar RNA host gene 12 promotes renal cell carcinoma progression by modulating the miR-200c-5p/collagen type XI alpha1 chain pathway. Mol Med Rep. 2020; 22:3677-3686.
38. Zhang C, Ren X, Zhang W, et al. Prognostic and clinical significance of long non-coding RNA SNHG12 expression in various cancers. Bioengineered. 2020; 11:1112-1123.

Figures

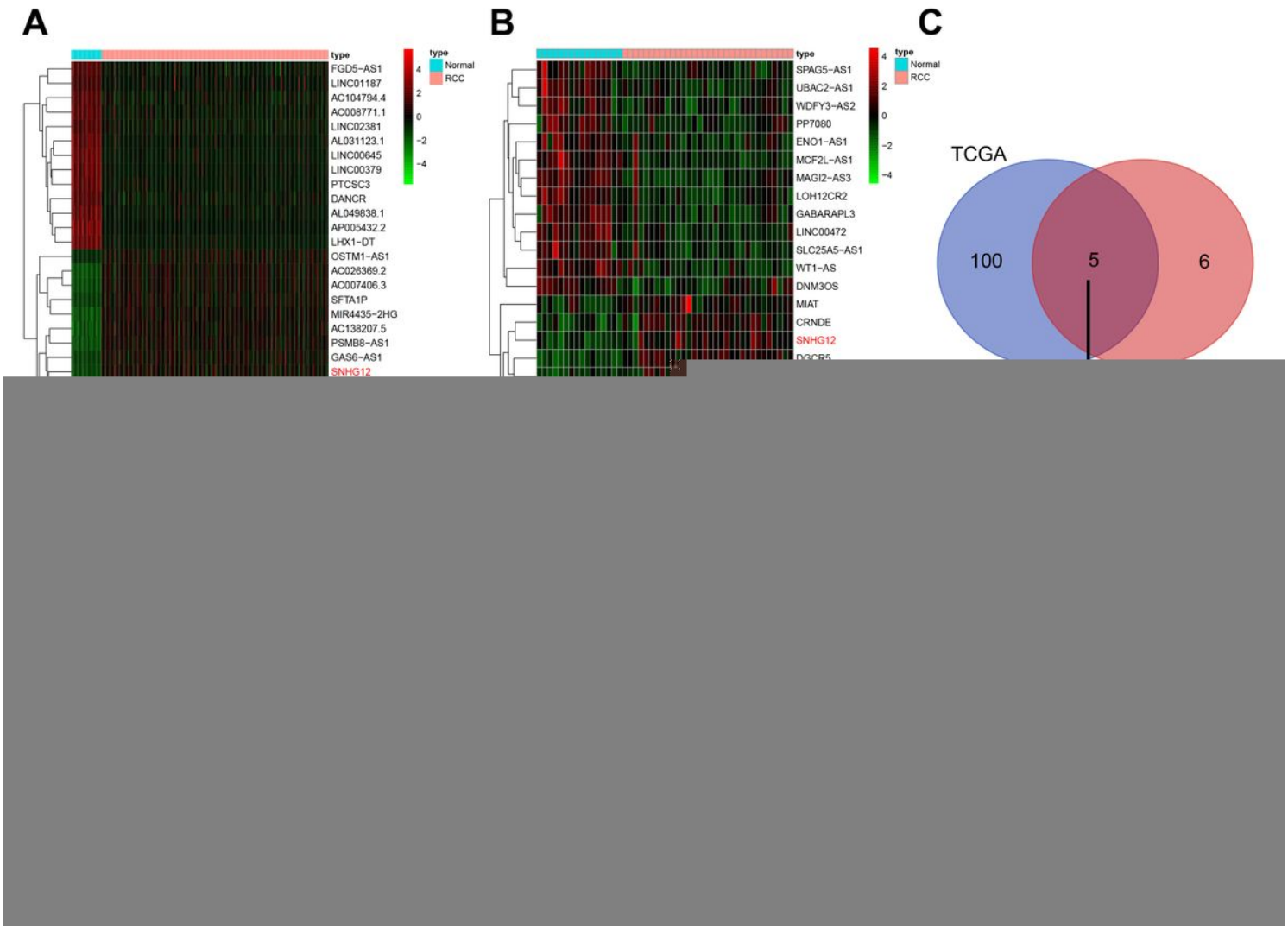

Figure 1

Differential expression of SNHG12 in RCC tissues and cells.

A: Heatmap of the first 30 differentially expressed lncRNAs between 535 RCC samples and 72 normal tissue samples from TCGA database. B: Heatmap of differentially expressed lncRNA between 32 RCC samples and 16 normal tissue samples in the GSE71963 dataset. C: Venn plot showing the overlapping regions of the up-regulated lncRNAs in the TCGA and GSE71963 datasets. D: Kaplan-Meier overall survival curve of RCC patients with high and low SNHG12 expression in the TCGA database. E: RT-qPCR analysis of SNHG12 expression in RCC tissues and paracancerous tissues (N=46). F: RT-qPCR analysis of SNHG12 expression in HK-2 and RCC cell lines. * P<0.05.** P<0.01. All experiments were repeated three times.

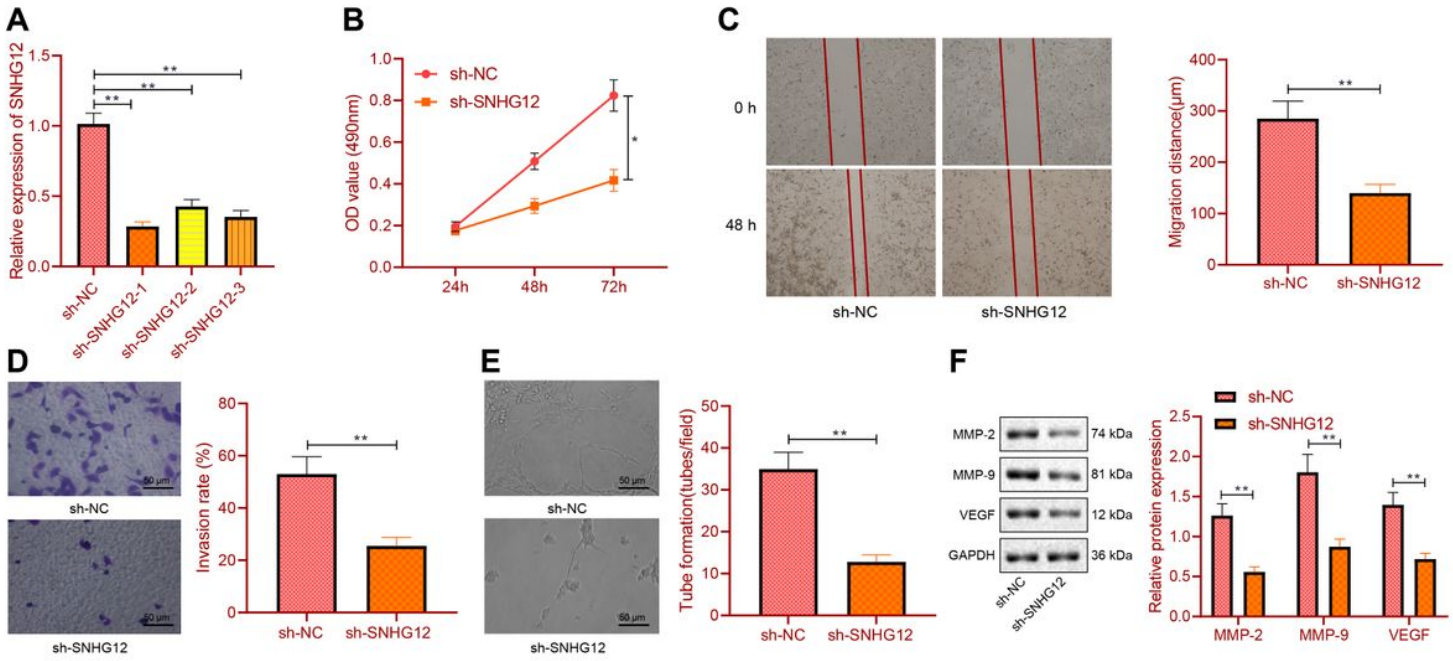

Figure 2

The effect of knocking down SNHG12 on RCC.

A: The knockdown efficiency of SNHG12 was tested by RT-qPCR. B: The proliferation ability of RCC cells was detected by CCK-8 method. C: Cell migration ability was detected by wound healing test. D: Cell invasion ability was analyzed by Transwell assay. E: The ability of knocking down SNHG12 on capillary-like tube formation of HUVECs *in vitro*. F: Detection of MMP-2, MMP-9, and VEGF protein expression by Western Blot. *P <0.05, **P <0.01. All experiments were repeated three times.

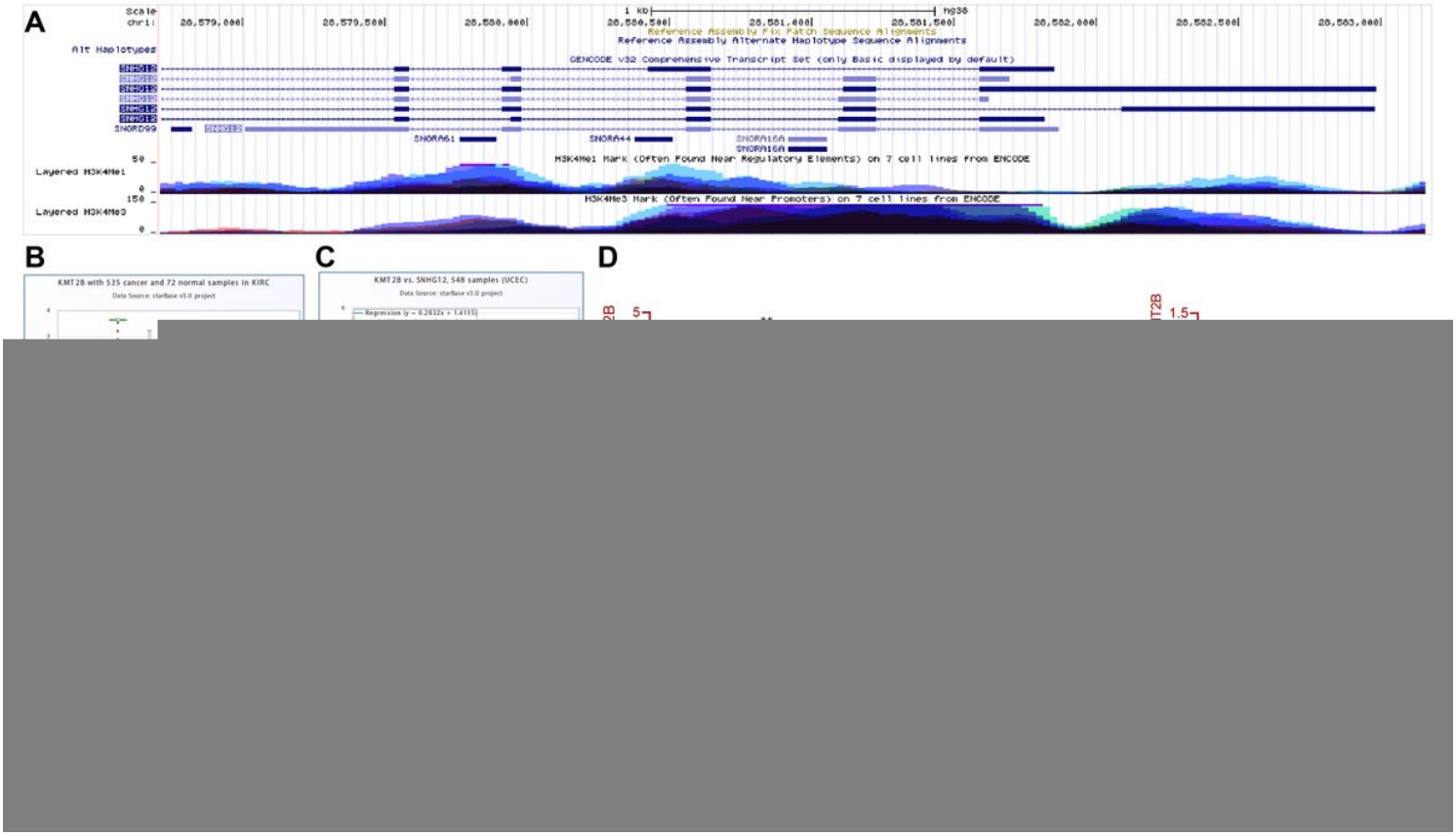

Figure 3

The effect of KMT2B on H3K4me3 modification in the promoter region of SNHG12.

A: The enrichment of H3K4me3 modification in the promoter region of SNHG12 was analyzed by the UCSC database. B: The expression of KMT2B in RCC was analyzed by ENCORI database (RCC=535, Normal=72). C: Through the ENCORI database, the correlation between KMT2B and SNHG12 in RCC was analyzed. D: The expression of KMT2B in RCC tissues was detected by RT-qPCR and Western Blot. E: The expression of KMT2B in RCC cells was detected by RT-qPCR and Western Blot. F: The expression levels of KMT2B and SNHG12 after knocking down KMT2B were detected by RT-qPCR. G: After knocking down KMT2B, ChIP was used to detect the enrichment of H3K4me3 in the promoter region of SNHG12. *P <0.05, **P <0.01. All experiments were repeated three times.

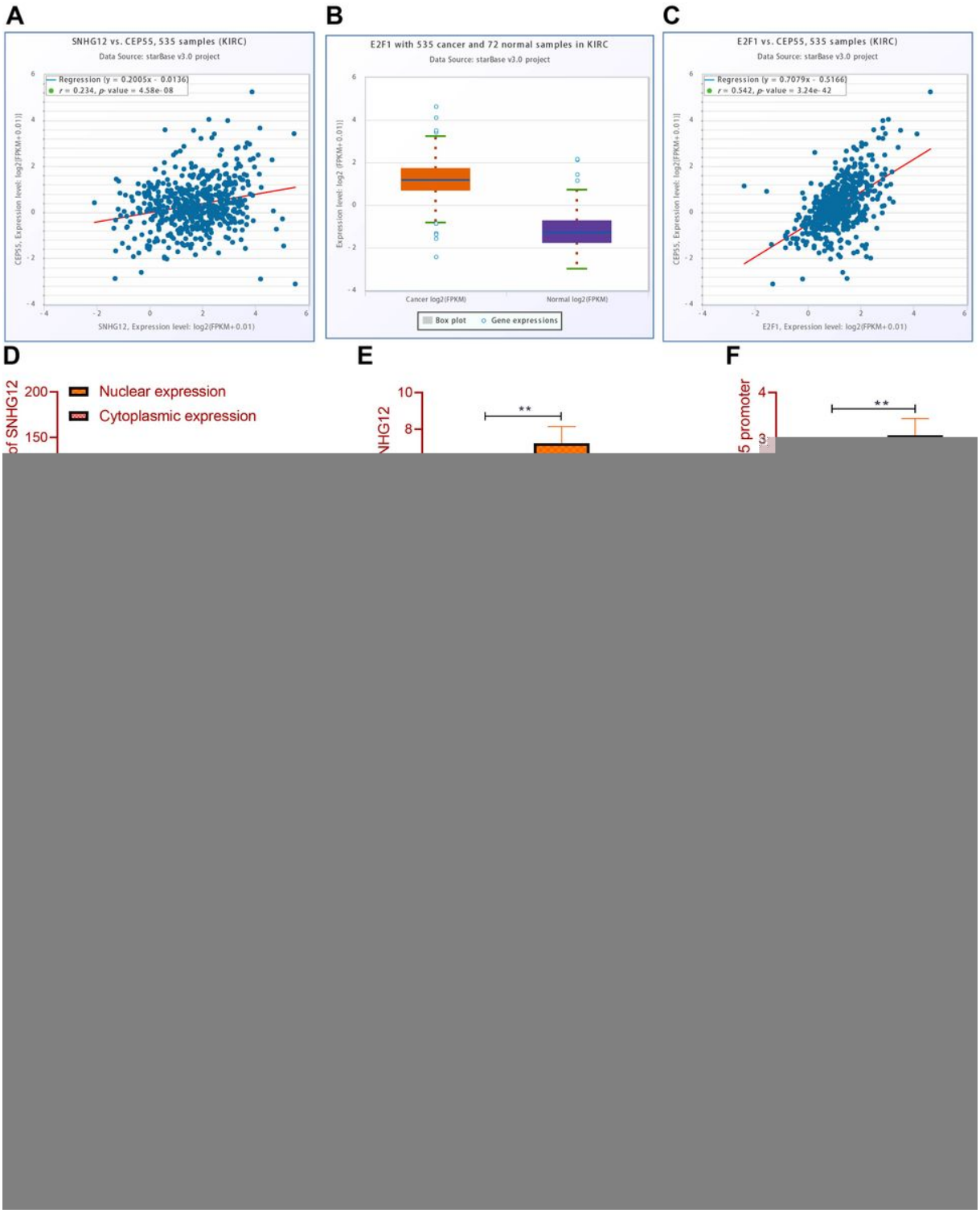

Figure 4

SNHG12 recruits transcription factor E2F1 to affect CEP55 transcription.

A: The correlation between SNHG12 and CEP55 in RCC was analyzed through ENCORI database. B: The expression of E2F1 in RCC was analyzed through the ENCORI database (RCC=535, Normal=72). C: The correlation between E2F1 and CEP55 in RCC was analyzed through the ENCORI database. D: The level of SNHG12 in nuclear and cytoplasm was analyzed by RT-qPCR. E: The binding of SNHG12 and E2F1 was

detected by RIP. F: Detection of E2F1 binding to the CEP55 promoter region by CHIP. G: After overexpression of SNHG12, the binding of E2F1 to the CEP55 promoter region was detected by CHIP. H: The binding of transcription factor E2F1 to the promoter region of the target gene CEP55 was detected by dual luciferase reporter assay. I: Three sites in the promoter region of CEP55. J: The expression of CEP55 in each group was detected by RT-qPCR. *P <0.05. All experiments were repeated three times.

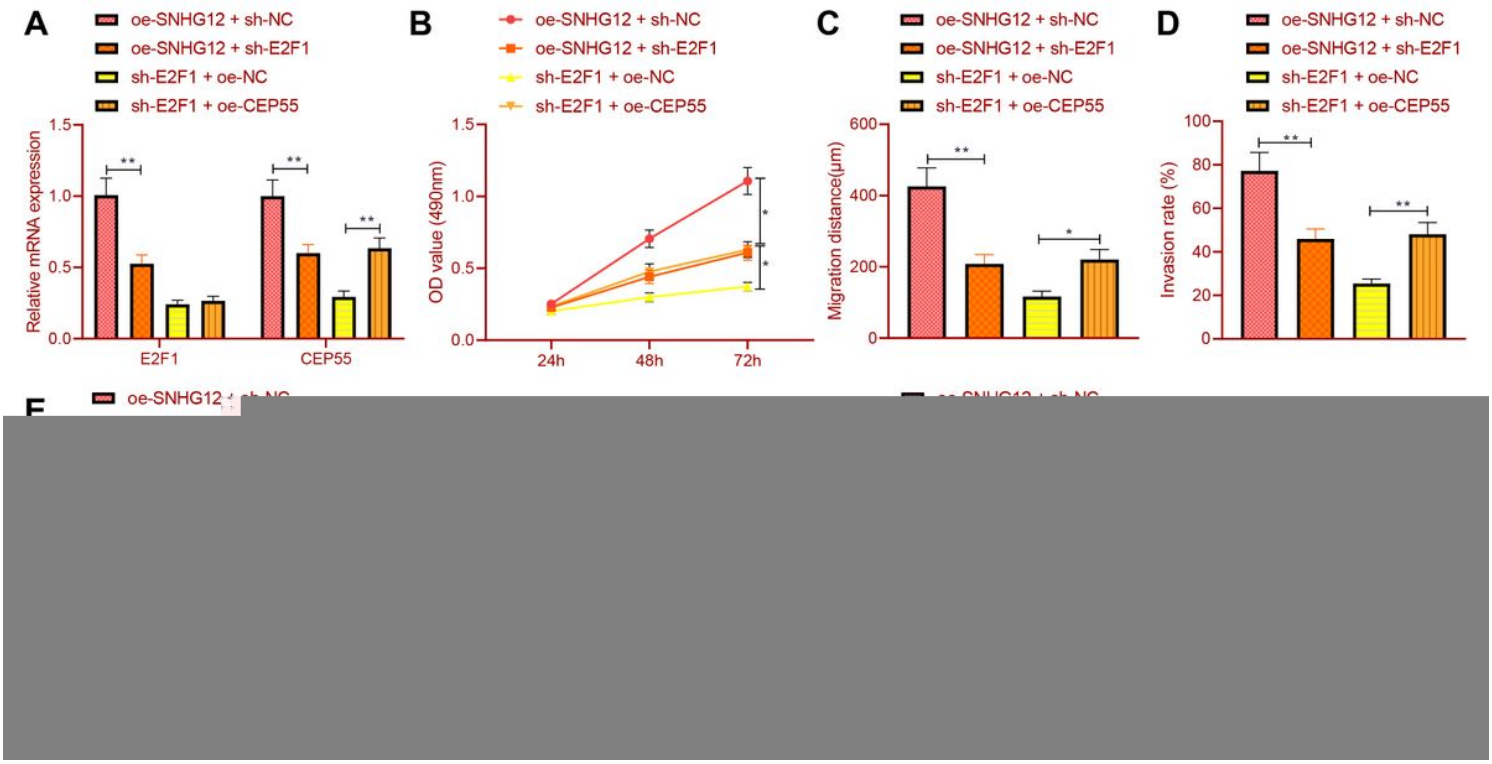

Figure 5

The effect of SNHG12/E2F1/CEP55 on RCC cell proliferation, migration, invasion and HUVEC angiogenesis.

A: The expression of E2F1 and CEP55 in each group of cells was detected by RT-qPCR. B: The proliferation ability of RCC cells was detected by CCK-8. C: Detection of cell migration ability by wound healing test. D: Detection of cell invasion by Transwell assay. E: Analysis of the angiogenesis ability of HUVECs by *in vitro* capillary-like tube formation. F: Detect the expression of MMP-2, MMP-9 and VEGF by Western Blot. *P <0.05. All experiments were repeated three times.

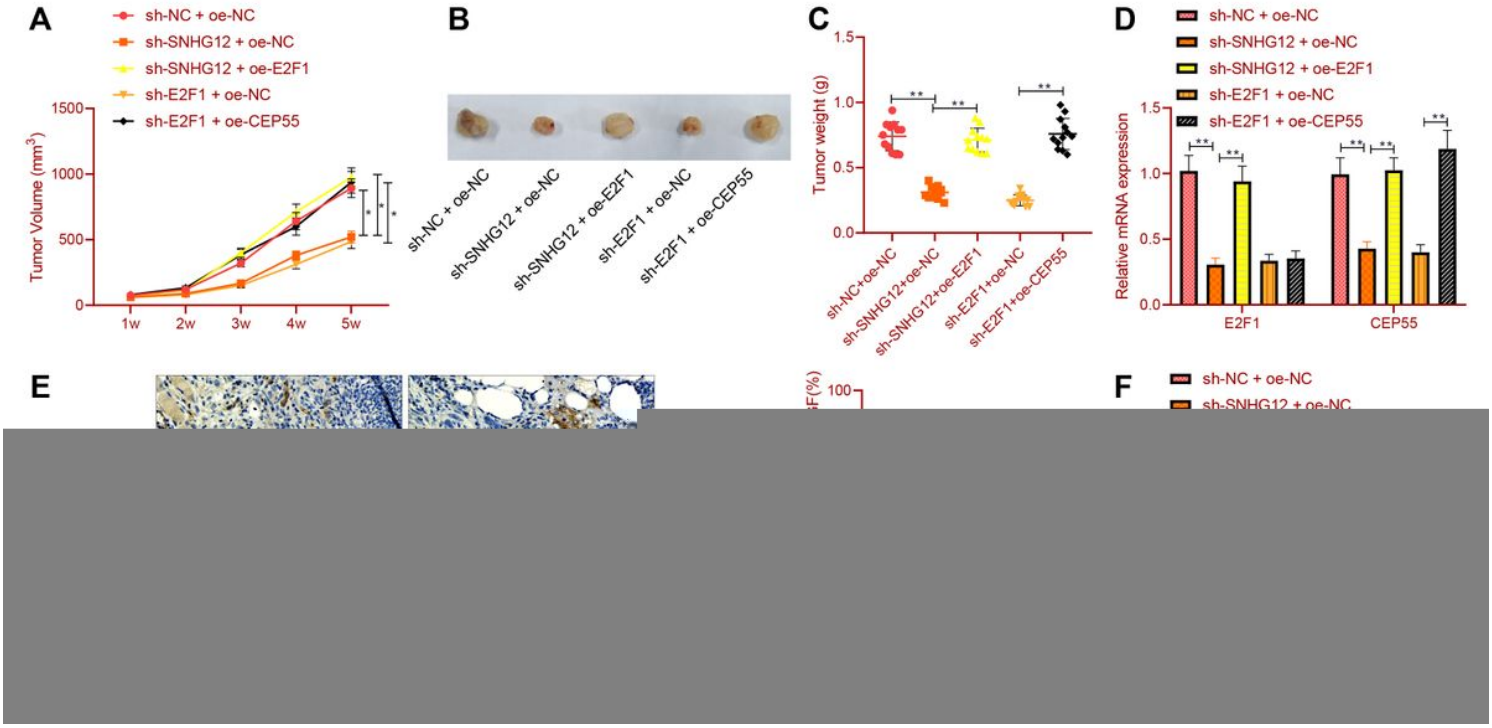

Figure 6

The effect of SNHG12/E2F1/CEP55 on RCC growth and angiogenesis *in vivo*.

A: Analysis of tumor volume. B: Gross morphology of tumors. C: Analysis of tumor weight (N=12). D: The expression of *E2F1* and *CEP55* mRNAs in tumor tissues was detected by RT-qPCR. E: The expression of VEGF in tumor tissue was detected by immunohistochemistry. F: Detection of the expression of MMP-2, MMP-9 and VEGF in tumor tissue by Western Blot; *P <0.05, ** P <0.01. All experiments were repeated three times.

Figure 7

Schematic diagram of the mechanism of SNHG12 in RCC.

KMT2B up-regulates SNHG12 through the modification of H3K4me3, which in turn recruits the transcription factor E2F1, and ultimately promotes the expression of CEP55, and related factors such as VEGF, MMP-2 and MMP-9.